33RD CONGRESS
OF THE INTERNATIONAL COUNCIL
OF THE AERONAUTICAL SCIENCES
STOCKHOLM, SWEDEN, 4-9 SEPTEMBER, 2022

ICAS 2022 SWEDEN

Fatigue Crack Propagation in Additively Manufactured Polymer Parts

El Fazani Hayat[1], Coil Jason[2], Laliberté Jeremy[3]

[1,2,3]Carleton University, Department of Mechanical and Aerospace Engineering, Ottawa, Ontario, K1S 5B6, Canada

hayatelfazani@cmail.carleton.ca

Abstract

This study is aimed to assess the fatigue performance of additive manufacturing (AM) parts for aerospace application. This will lead to the improvement of AM part designs. A computer aided design (CAD) program is used to design groups of fatigue coupons with dimensions specified in the ASTM D3479 Standards. These specimens are made from a commercial Polymer, acrylonitrile-butadiene-styrene (ABS) P430. A Stratasys SST 1200es fused deposition machine was used to manufacture flat AM coupons. The specimens were also built in different angles of orientations (0°, 22.5°, 45°, 67.5° and 90°). The purpose of this research is to investigate the material behavior under different fatigue loading conditions. It is essential to understand the mechanics underlying the failure process to ensure a high quality of AM end product. Fatigue analysis was conducted and both fatigue initiation and propagation will be investigated, with the focus will be on crack initiation. The proposed test matrix explains the number of tested coupons, where 21 flat specimens are tested with a degree of orientations (0°, 22.5°, 45°, 67.5° and 90°). The fatigue test for this paper is based on measuring the crack length of AM specimen caused by low cyclic fatigue loading. An optical microscopy is used to track the crack upon initiation. Also, multiples cracks are measured within the same AM specimen. The relation between crack length, for individual crack and multiple cracks, versus the number of fatigue cycles is obtained. In addition, the variation of fatigue life with specimens build orientations is discussed. This study will also identify which fatigue test methods are suitable for polymer AM components.

Keywords: Additive Manufacturing; Fatigue test; Crack length; Crack propagation; Build orientations.

1. Introduction

Additive Manufacturing (AM), commonly known as 3D printing, is the process of building a part layer by layer with material deposition until the final product has been manufactured. The American Society for Testing and Materials (ASTM) 2792-12 described the Additive Manufacturing technology as "processes of joining materials to make objects from 3D model data, usually layer upon layer, as opposed to subtractive manufacturing fabrication methodologies" [1]. In contrast to the subtractive manufacturing method, where an object is machined down from bulk material, the AM process starts with a 3D model created using a computer-aided drawing (CAD) software. The model will be transformed into STL format which is then imported by an AM software, a process described as computer-aided manufacturing (CAM) [2]. Cura software was used to slice the CAD model into multiple layers. Then the AM machine manufactured these layers one by one to create final part.

Additive Manufacturing technology has been introduced since the 1980s [3][4][5]. It has been taking strong attention from industry, research, and academia [6][7]. Aerospace companies and researchers are investing lots of money and time in AM to uncover its full potential applications. Additive Manufacturing technology offers important advantages including the ability to manufacture parts with complex geometries and less weight [6][7][8] than previously capable. This fits very well with the aerospace industry where a lightweight design is advantageous. The AM method also decreased the final product lead-time, and lowered the cost compared to traditional manufacturing techniques [9][7]. In addition, AM promises a dramatic reduction in inventory and warehousing [10][11].

It was argued that polymers have limited usage for space flight [12]. The idea around holding up the polymer production tools was also discussed in [7]. The challenges facing polymer applications were highlighted and it was recommended that specific needs for the aerospace industry must be fulfilled through further research. The lack of suitable fatigue data of AM polymers was addressed in [13]. On the contrary, some researcher argued that there were great opportunities for thermoplastic materials for current aerospace applications. It was suggested that the plastic parts can be utilized for non-structural applications including environmental control system ducts, protective covers and cockpit parts [7]. Therefore, some applications of polymer materials have already emerged. As an example, Boeing installed AM plastic air-cooling ducts for the environmental control system of the F-18 Super Hornet fighter jet [5].

1.1 Background on Fatigue Analysis

Although, AM technology has brought great advantages, there is a current need to further study the material behavior of AM parts. The lack of research publication on fatigue analysis for AM polymer parts manufactured by FDM technique was discussed in [14][15]. The fatigue crack propagation behavior for polymers continues to be an active area of study in the aerospace industry [16]. A study compared the fatigue life of ABS polymer made by AM technology with the bulk precursor material [17]. The results demonstrate that AM polymer has a significant lower fatigue life which indicates a challenge in applying AM polymer parts into functional products and the application into real service conditions [18]. ABS 3D printed polymers have very limited fatigue characteristics, which limits their feasibility for application in the aircraft structure [7]. The researcher in [19] discussed the fatigue fracture for polymer material for the 3 stages of fracture; crack initiation, crack propagation and final fracture. Alternatively, Nicholas Choo-Son the Director, Business Development at Marsh Brother Aviation argues that the application of polymer material can revolutionize the aviation industry. For example, it will permanently reduce the need for applying grease in the landing gear. Marsh Brothers Aviation company [20] has recently accomplished the Transport Canada and FAA STC approval for installing a complete Aerostar aircraft landing gear grease free bushing as shown in Fig (1). The application of polymer materials for aerospace structures was also discussed in [21].

Figure 1 - Polymer landing gear bushings [20].

1.2 Objectives

The objective of this paper is to study the application of damage tolerance and fatigue evaluation of polymer parts made by additive manufacturing technology. Therefore, the fatigue characteristics of polymer parts made by FDM technique was discussed. This includes the influence of building orientation on the fatigue life of the AM parts. The crack growth in AM polymer specimen was also monitored.

2. Methodology

The following sections will include the specimen design and manufacturing, including the specimen dimensions. Also, a description of the equipment used in this experimental will be provided along with test set up and procedure.

2.1 Specimen Design and Manufacturing

The material used to manufacture AM parts is a commercial polymer acrylonitrile-butadiene-styrene (ABS) P430. The selection of ABS was based on its low cost and common use in fused deposition modelling (FDM) technology [22]. ABS is one of the most widely used industrial thermoplastic in automotive, aerospace, medical, and many other applications [2]. This thermoplastic polymer will soften when heated during the extruding process, allowing it to take form of a part, which then hardens when it returns to room temperature. The softened filaments will bind each other and weld to previous layers of material [23]. The mechanical and thermal properties for ABS – P430 were published by the Stratasys 3D printing company and it can be found in [24]. The fatigue coupon with dimensions specified in the ASTM D3479 Standards [25] shown in Fig (2) was used to design the specimen. In this study, the flat specimens were manufactured in different angles of orientations (0°, 22.5°, 45°, 67.5°, and 90°). The process of slicing the AM model into layers by using Simplify 3D slicing software is illustrated in Fig (3). The tool path for manufacturing the AM fatigue coupon by FDM is illustrated. The layout of the flat samples and the manufacturing process are illustrated in Fig (4).

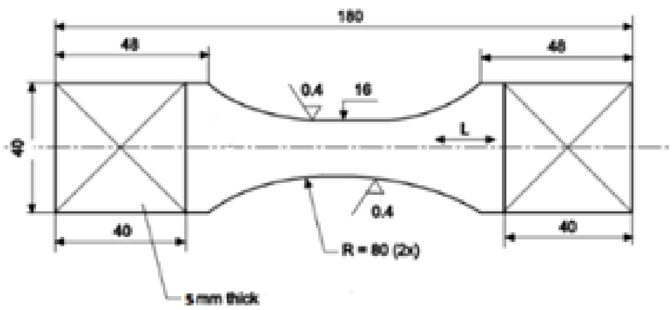

Figure 2 - Fatigue coupon dimensions use for fatigue crack initiation tests with low K_t [25].

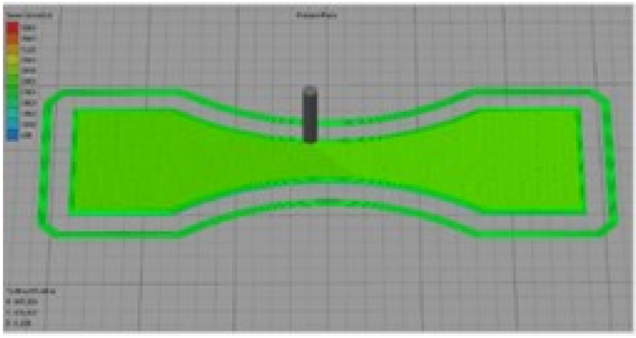

Figure 3 - Tool path for building AM fatigue coupon using Simplify 3D.

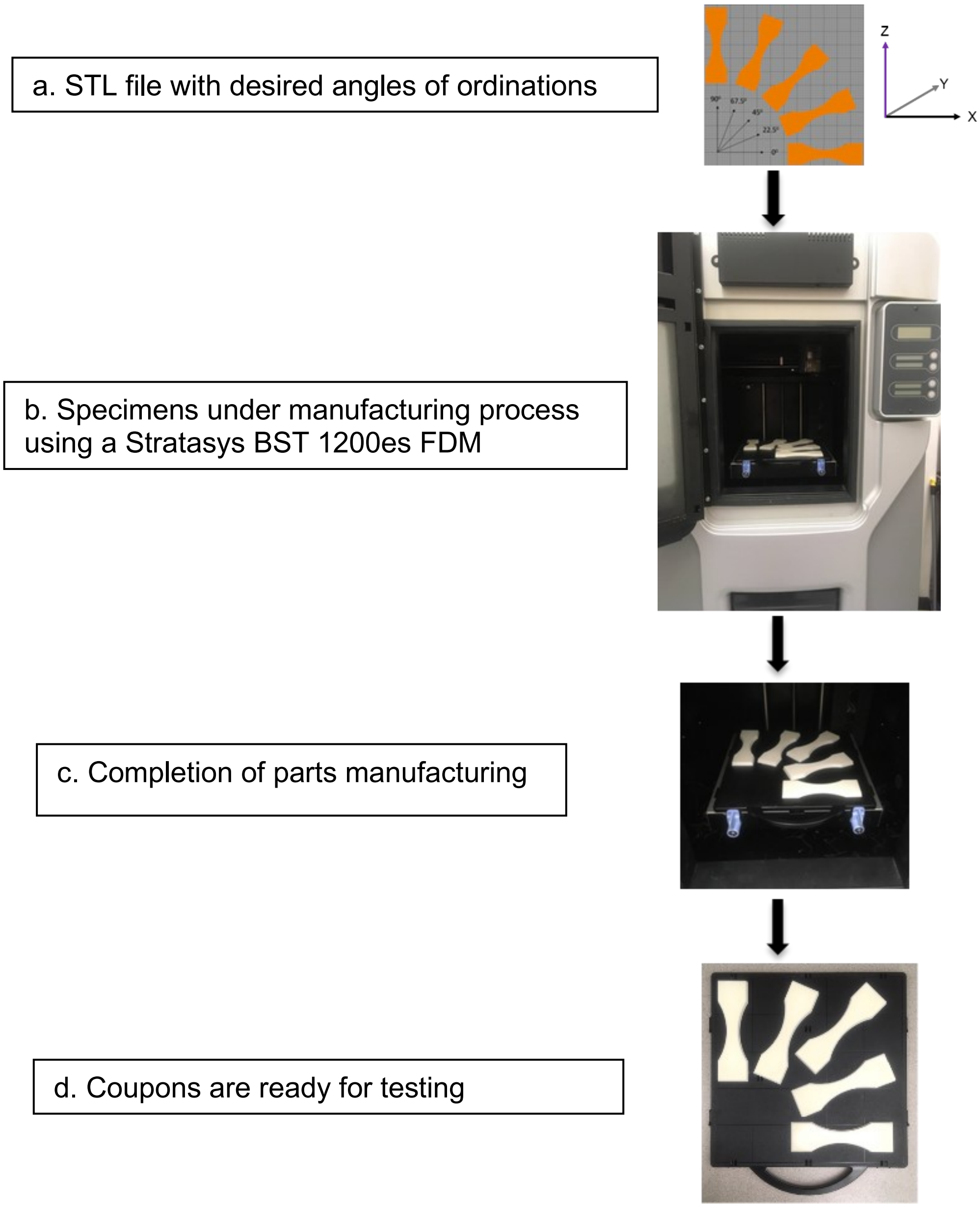

Figure 4 - The manufacturing process of AM fatigue flat specimens.

2.1.1 Specimens Measurements

A digital fractional caliper was used to measure the true dimensions of AM fatigue specimens as shown in Table (1). The printed specimens were found to be within an accuracy of +/- 0.01 mm. This step is essential as the temperature variations may lead to deviance in the dimension of AM polymer part. There are other parameters that may have an impact on the finished part. This includes the compatibility of STL file with the AM machine, the manufacturing process, the printing speed, and layer thickness. However, this paper does not consider the effect of those parameters on the specimens. All specimens were weighed immediately after the manufacturing process using scales with accuracy of 0.0001 g. The specimens were stored in a zip-lock bags at room temperature and they were ready for testing. Table (2) shows the mass measurement for fatigue coupon built on flat.

Table 1 - Measurements for fatigue coupons.

Build orientations (degree)	Average full length (mm)	Average thickness (mm)	Average width (mm)	Average cross-sectional area (mm^2)
0°	140.03± 0.06	5.30± 0.06	16.05± 0.01	85.01± 0.91
45°	140.16± 0.05	5.21± 0.08	15.98± 0.02	83.19± 0.99
90°	140.26± 0.04	5.23± 0.06	15.98± 0.03	83.60± 0.83

Table 2 - Mass measurements for fatigue coupons.

Build orientations (degree)	Mass (g)
0°	21.4213 ± 0.0001
45°	21.3501± 0.0001
90°	21.4121± 0.0001

2.1.2 Fused Deposition Modelling (FDM)

The American Society for Testing and Materials (ASTM) has developed a standard to organize AM processes into seven categories [1]. These classifications were based on the type of material used, the deposition technique, or the method at which the material is fused or solidified. In this paper, the specimens were fabricated based on Material Deposition Modelling (FDM). The workings of the FDM process is illustrated in Fig (5). A thermoplastic polymer filament, in this case ABS, is melted and extruded through the heated nozzle and placed on the building platform layer by layer. The process is then repeated until the final object is built. A support material is used to help hold the components shape during the manufacturing process.

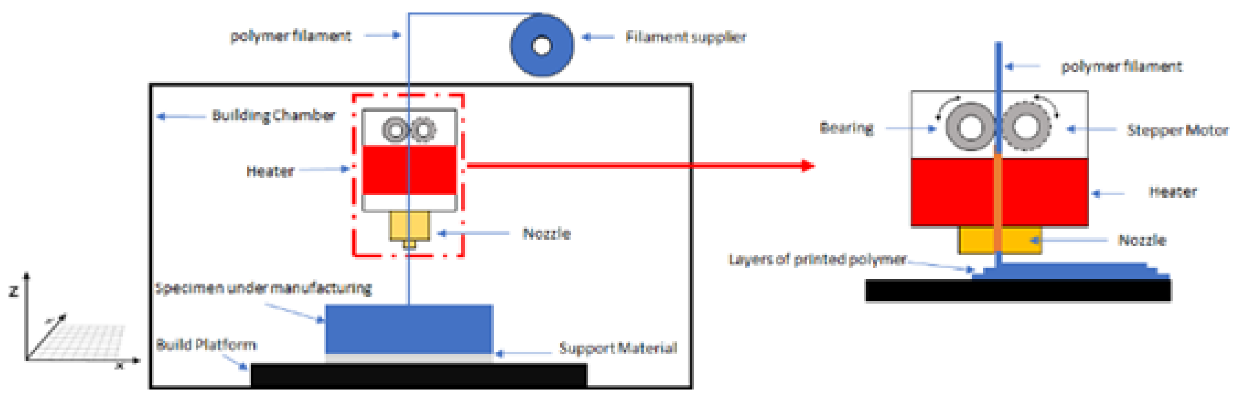

Figure 5 - Schematic of fused deposition modelling (FDM) Process.

A Stratasys SST 1200es FDM Machine was used to manufacture the specimens, as shown in Fig (4). The fatigue coupons were modeled using CAD software, which was then converted to STL file for FDM. The slicing software used was Catalyst EX 4.3. The build volume of this machine is 254 x 254 x 305 mm [24], a size which allows more than one coupon to be manufactured at the same time. As illustrated in Fig (6), the outer nozzle outer diameter is 0.95 mm and the filament diameter of ABS material is 1.75mm. The nozzle temperature is 230°C. The printing layer thickness of each specimen is 0.254 mm and the raster distance (path) is 0.44 mm. The interior setting of all specimens is "solid" model.

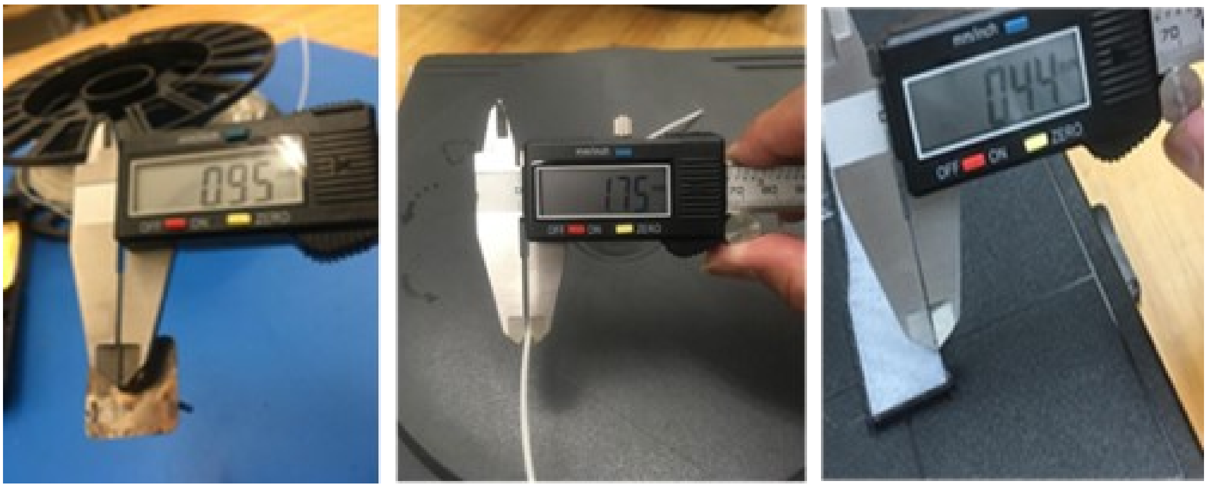

(a) (b) (c)

Figure 6 - a) Nozzle diameter b) filament diameter, c) raster distance.

2.2 Test matrix

The purpose of this paper is to study the effect of building orientations on the mechanical properties of AM polymers. More specifically, the goal was to investigate the fatigue performance of FDM components as a function of angle of orientations. A test matrix was used to keep track of the results for each orientation of the coupon. This research introduces the following test matrix with a total number of 21 coupons. Table (3) illustrates the minimum number of proposed fatigue testing.

Table 3 - Material Test Matrix

Sample Orientations (degrees)	Number of Samples Printed (on Flat)
0°	4
22.5°	3
45°	4
67.5°	3
90°	7
Total	21

2.3 Test Procedure

In this experimental study, the fatigue life of AM polymer components was to be determined. The fatigue failure of a part may start with a crack formation at a point of high stress concentration. This is then followed by crack propagation, which ultimately leads to total failure of the component. The equipment and test procedures are explained in the following sections:

2.3.1 Equipment

Fatigue testing was performed in the Structures Lab of the Mechanical and Aerospace Engineering Department at Carleton University. Table (4) shows a list of necessary equipment used for this experiment with a brief description.

Table 4 - List of equipment

Equipment	Description
Fatigue test specimens	A regular fatigue test specimen has three areas: the test section and two identical grip ends.
25 kN MTS load frame	Materials Testing System (MTS) machine with a maximum loading of 25kN
MTS software and a computer station	Enables the setup of test parameters and data acquisition
Travelling microscope	Used to observe and measure the cracks with an accuracy of (+/- 0.01 mm)
Point light source	Helps to illuminate the specimen to clearly identify cracks

2.3.2 Test Setup and Procedure

Following the ASTM standards, each specimen has two identical grip ends which are used to transfer the load generated by the MTS machine to the gauge section. To reduce the sources of errors in this test, two fences shown in Fig (7) were designed to help align the specimen vertically. The specimen was designed with two large and smooth radii reducing the possibility of stress concentrations that may cause premature specimen failure during cyclic loading. The specimen was gripped axially in the loading direction. The cross-hatched grips were used to fix the specimen with a gripping pressure of 400 Psi.

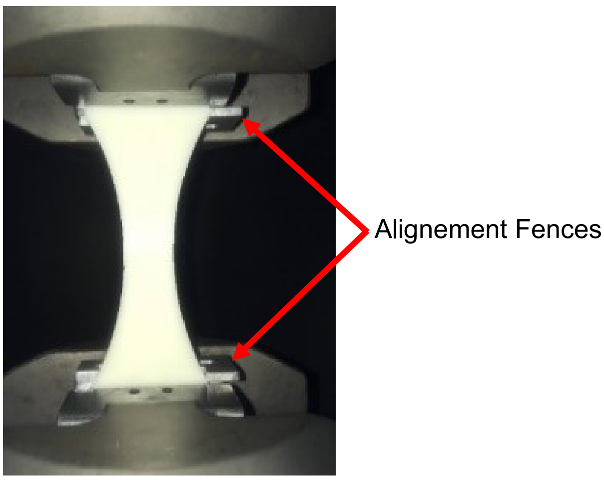

Figure 7 - Specimen aligned fences.

The basic fatigue tests refer to a test coupon that is subjected to a cyclic load. The frequency and stress amplitude applied during fatigue testing will cause the polymer to exhibit either thermal softening or cyclic crack growth [26]. In this research, the specimens were tested under sinusoidal tension-tension fatigue loading at a low frequency of 3 Hz, as shown in Fig (8). The maximum applied load was + 0.9 kN and the minimum applied load was zero. The selection of this type of loading condition was based on previous literature [17][27]. Testing the specimen at low frequency eliminates any heating effects due to the strains. It also avoids any bending that might occur from compression. In addition, if a compression load is applied, it becomes very difficult to accurately identify the crack length as the crack will be closed during compression. The undesired compression force may also lead to losing the features of the fracture surface, which are very important to the analysis. The test was conducted at room-temperature (approximately 21° C). The specimen surface was observed during loading and unloading. A small crack starts to form and initiate on the gauge length of the tested area.

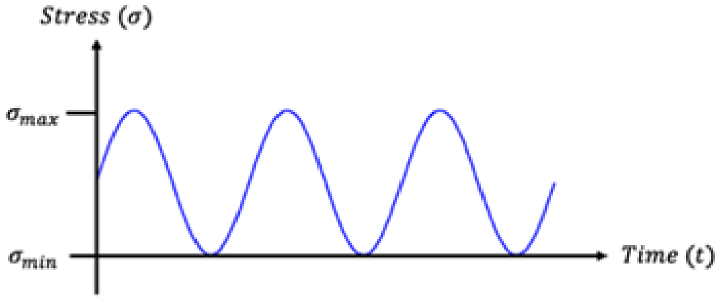

Figure 8 - Constant amplitude fatigue.

The chosen method of crack monitoring was to use travelling microscope, where the crack tip was monitored with a crosshair and with light point assistant as shown in Fig (9.3). The microscope travels parallel to the crack using a hand crank. The travel microscope has a digital measurement allows a crack measurement with an accuracy of 0.01mm [28]. The crack propagation was monitored to critical dimensions or until the specimens fail [29]. The first specimen was cycled for 300 cycles and then stopped. The gauge area was carefully observed by using the travelling microscope to identify the cracks. All cracks and their respective lengths were measured and recorded. Small cracks formed both on and inside the surface as shown in Fig (9.5). The crack initiation was due to high stress concentration points, also called stress raisers. After crack initiation, continual loading of the stress concentration with additional cycles leads to a gradual crack propagation. The crack becomes unstable. A sudden quick failure then occurs as shown in Fig (9.7).

These steps were repeated until the desired cycle number is reached or until the specimen fails. The same steps were repeated for all specimens in the test matrix. The number of cycles at the final failure was recorded and all data saved for analysis. The cracks properties, crack shape, observations and measurements are illustrated in Fig (10). For example, Fig (10.1) shows multiple cracks (i.e. branching) which were initiated at the edge of the testing area, each with an approximate short length of 0.2 mm. Fig (10.2) displays two cracks, where one was initiated from the surface and the other which initiated from an inside location (inclusion). Continuing loading and unloading of the specimen over time leads to an increase of the stress concentration around the crack tip. This spot is known as the plastic zone. This area is elongated and increased in size which causes a gradual crack propagation with each stress cycle.

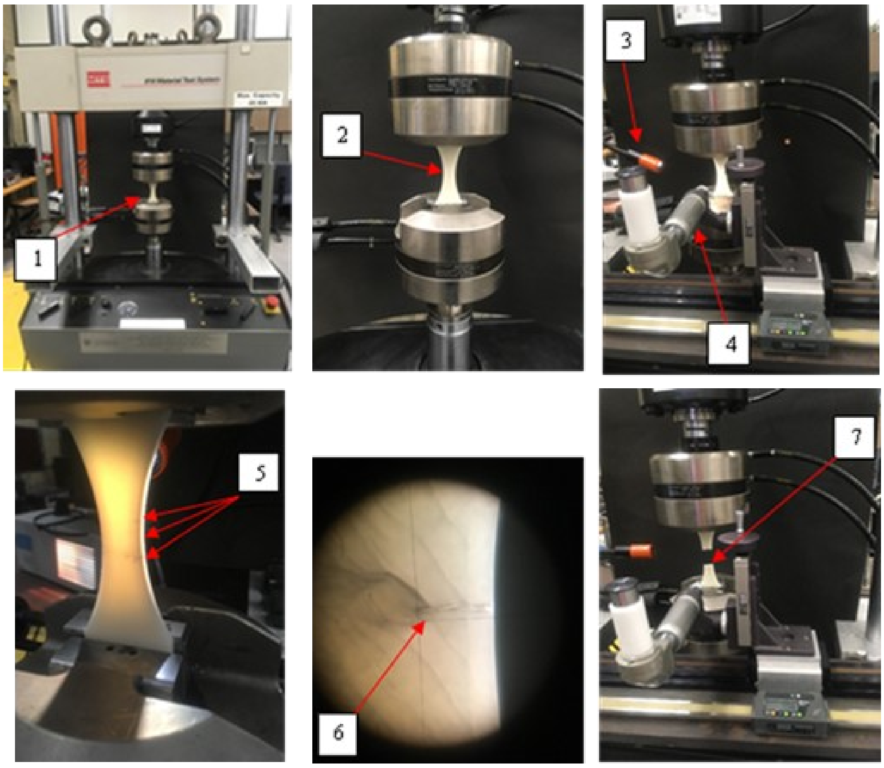

Figure 9 - Fatigue testing procedure: 1. specimen mounted at 25 kN MTS load frame, 2. under fatigue testing, 3. light source 4. travel microscope, 5. multiple cracks, 6. single crack length measurements, 7. specimen at failure.

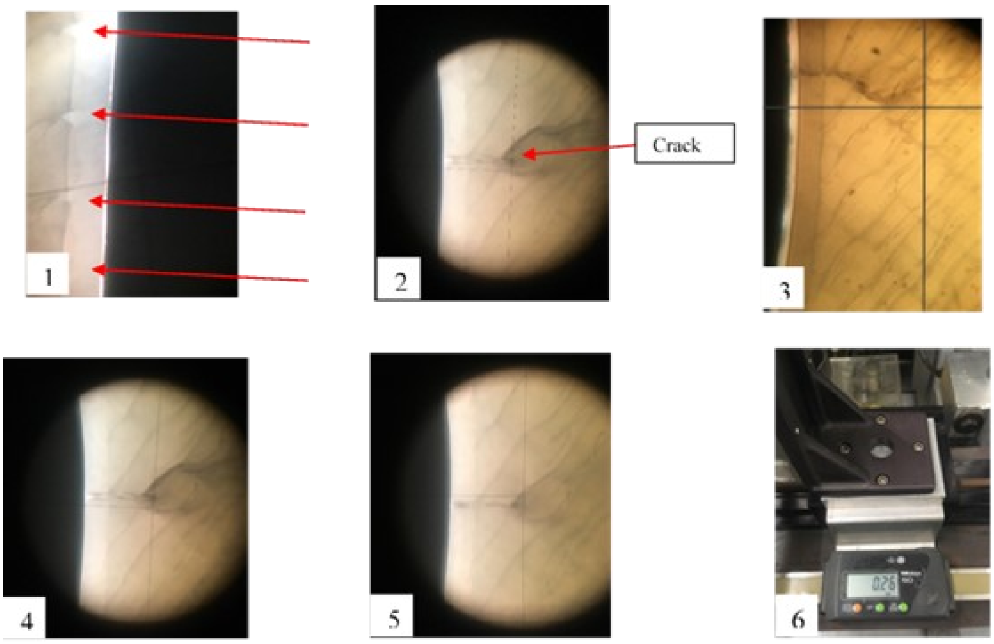

Figure 10 - Fatigue crack characters: 1. cracks initiation 2. edge crack and a central crack formed to crack one individual crack, 3. crack propagation, 4. open cracks under tension loading, 5. crack at zero load, 6. microscope digital reading in mm.

The travel microscope was able to translate in three directions as shown in Fig (11): right to left, up to down, and front to back. This was done to get the right focal distance, allowing the microscope to see the crack clearly. The crosshair center at the microscope lens was pointed at the crack tip, followed by moving the microscope parallel to the crack from the crack tip to the crack mouth for edge crack and from to tip to tip for a crack inside the specimen. The crack length was then obtained from the digital measurement of the movement of the microscope. The number of cycles associated with the crack measurements was recorded as well as the applied loads during the measuring. Fatigue cracks are in most cases oriented perpendicular to the loading direction as shown in Fig (10.5). The speed of an individual crack propagation can be influenced by other cracks surrounding a single crack. It is normal for multiple cracks under cyclic stress fluctuations to grow and come together to form a single long crack as shown in Fig (10.3). This crack then becomes unstable and a sudden quick failure will occur which will separate the specimen into two parts as shown in Fig (9). The number of cracks with its associated cycles was also reported for later analysis.

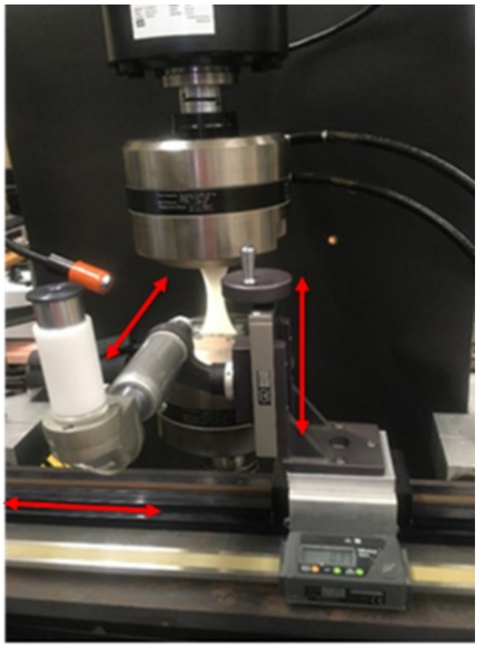

Figure 11 - Travelling microscope movement.

A schematic of a typical crack features with different shapes and branching for a single crack is shown in Fig (12). Figures (10.1), (10.2), (10.3), and (10.4) show cracks with shapes of branched, bilinear, winding, bend and straight, all of which were clearly observed at the current fatigue experiment.

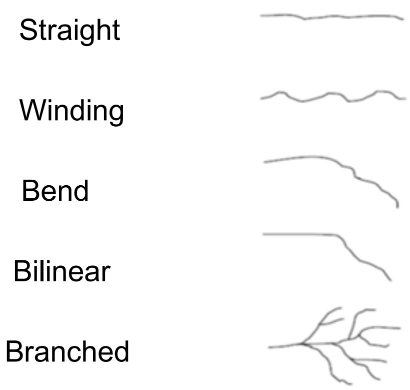

Figure 12 - Schematic of typical crack features, adopted from [30].

3. Results and Discussion

There is a strong relationship between the angle of orientation, the crack shape, and the final failure mode for each specimen. The failure modes for a group of flat specimens are presented in Fig (13). It was obvious that the failure modes for specimens built on the flat orientation have almost a winding fracture shape which was a result of single or multiple cracks with a winding shape. This can be seen in Fig (13.1) a sample with 90° build orientation. The failure mode of AM parts was varied because each specimen has its own variations in the unique angle or orientations, the gaps between the infill, and even variation in the extruder failing. Even though those parameters are outside the scope of this paper, it is essential to consider them in analyzing the fracture surface as it provides critical information on the material behavior and performance.

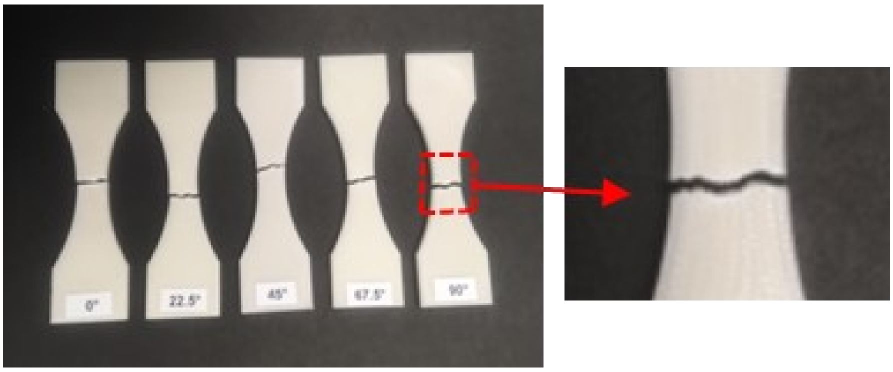

Figure 13 - Failure modes of flat specimens 1. building orientations (0°, 22.5°, 45°, 67.5° & 90°), 2. zoomed specimen with 90° angle of orientation.

This section discusses the results of the fatigue experiments for AM parts made from ABS polymer material. It includes the investigation of the effect of cyclic load on fatigue crack both at initiation and propagations. Through the results, the relation between individual crack lengths versus the number of cycles was obtained. Also, the influence of fatigue life on the cumulative of multiple cracks lengths, within a specimen, was examined. In addition, the effect of AM parts building orientations variations on the number of accumulated fatigue cycles was experimentally analyzed.

3.1 Fatigue analysis for flat specimens

The crack measurements obtained in this experiment was to be examined as a function of fatigue cycles. The curve shown in Fig (14) represents the crack propagation versus the number of cycles accumulated over time for one individual crack. This curve is known as a - N curve, where a is the typical crack length and N is the number of fatigue cycle. This relationship was generated for AM specimen built with 0° angle orientation. As illustrated, the shortest crack measured for this specimen at initiation was 0.12 mm at around 300 cycles. By accumulating more cycles, the crack continued to propagate, the length of which was continually measured. The total number of measurements for this test was planned such that 11 data points would be shown as in Fig (14). Based on observation, after 2000 cycles the crack becomes unstable and grows very fast in comparison to the early stages of this test. The last crack measurement was at 2250 cycles, with a recorded length of 4.8 mm. Then more cycles were added which will increase the crack speed until the final failure. This specimen was failed at a number of 2889 of cycles.

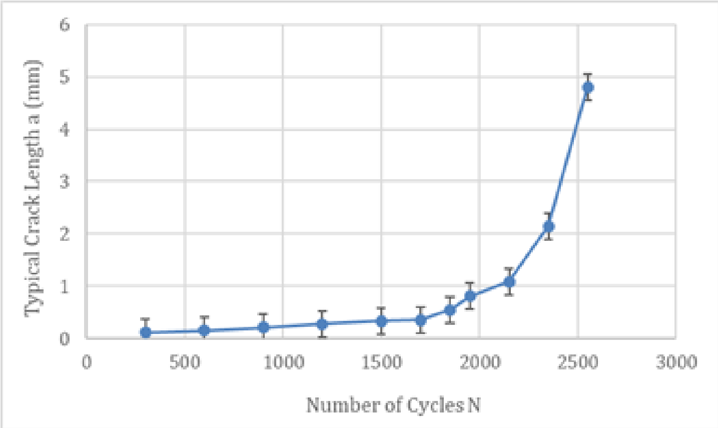

Figure 14 - Typical crack length versus the number of cycles for a specimen manufactured with 0° angle of orientation.

It is critical to study the effect of loading on not just one individual crack but also on the accumulated cracks. All the crack measurements were taken at tension between 0.88 kN and 0.9 kN, as shown in Fig (15). As discussed previously, the cracks in the damaged area were also monitored during cyclic loading. The crack lengths were recorded for 10 cracks in 4 selected specimens. As presented in the test matrix, the 4 specimens were manufactured in flat with 0° of orientations. The results presented in Fig (16) explains the relationship between the crack lengths of the accumulated cracks against the number of cycles of the 4 specimens fabricated in 0° angle of orientation. Each data point in this figure represents the summation of crack length measured at the specified number of cycles. For example, time measurements for specimen 4 was taken 11 times. They were taken every 300 cycles, up to 2550 cycles. The specimen failed at 2889 cycles. The initial accumulated crack lengths at 300 cycles was 1.5 mm, and the last measurement was taken where a group of 10 cracks measured at 2550 cycles. The same procedure was applied for the other 3 specimens, 0° - 1, 0° - 2, and 0° - 3, shown in this Fig (16). The cycles at which the measurements taken was not always the same, but the results show a great consistency of crack measurements for all 4 specimens. The total accumulative crack lengths for specimens 0° - 1, 0° - 2, 0° - 3, and 0° - 4 shown in Fig (16) were 12.92 mm, 13.87 mm, 13.94 mm, and 14.1 mm, respectively

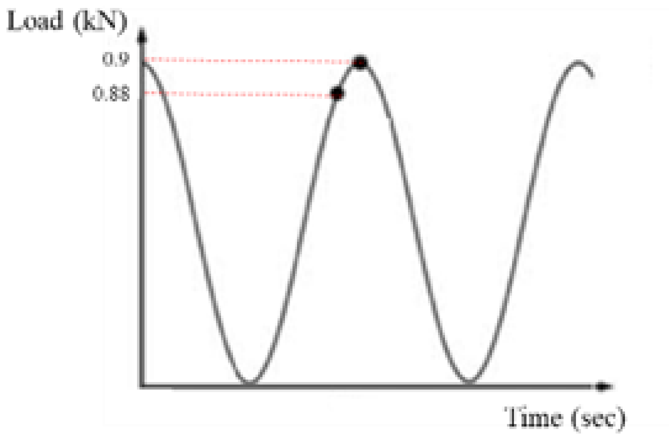

Figure 15 - Cyclic load at crack measurements.

.

In Fig (17), 10 cracks were monitored within each of the 4 specimens which were built in 45° orientations. The total crack lengths were plotted as a function of the number of cycles. The exhibited data demonstrates a range of accumulated crack lengths, with the minimum crack length measured at 5.69 mm for part 45° - 2 and maximum crack length measured at 8.2 mm for part 45° - 4. This means that the crack growth for specimens manufactured with 45° orientations was slower than specimens built with 0° printed orientations. Seven AM polymer specimens were tested with 90° build orientations. The collected crack measurements for multiple cracks versus the number of fatigue cycles are presented in Fig (18). The speed of crack propagation was similar for all specimens. However, the number of time measurements varied. For instance, the number of measured times of specimen number 7 was 15 while for part number 2 it was 4. The maximum cumulative cracks length was recorded to be 5.2 mm for specimen number 7 at 2300 fatigue cycles. This value was much lower than the results of the other two groups of specimens manufactured with 0° and 45° orientations. Therefore, the variation in crack lengths between the 3 groups can perhaps be attributed to the manufacturing method. This includes the layout and the variation of build orientations. As well, the difference in specimen's density can influence the part response to the fatigue loading.

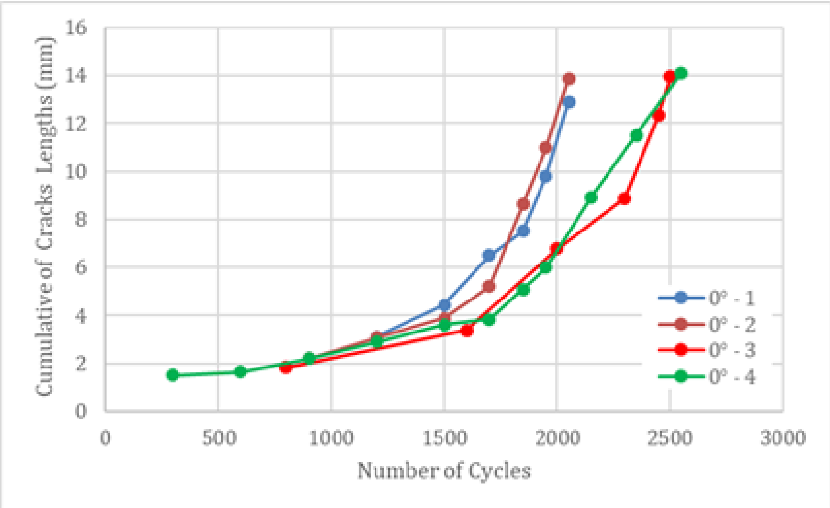

Figure 16 - The cumulative cracks lengths versus number of cycles for 4 specimens manufactured in 0° angle of orientations.

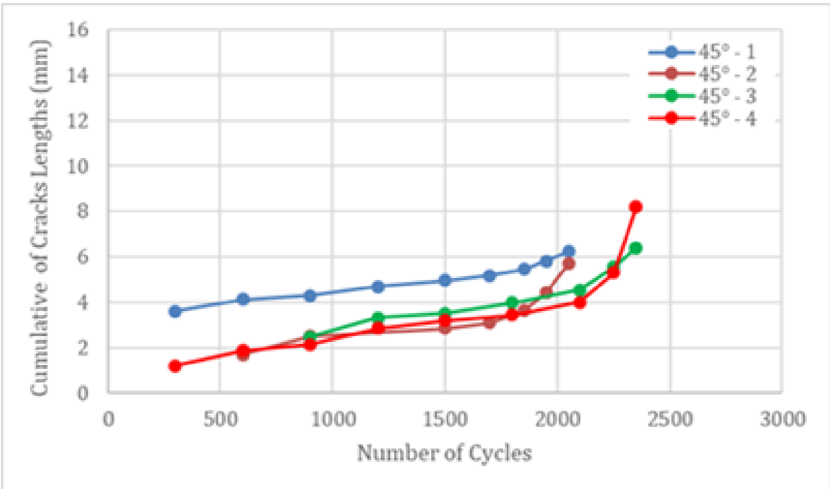

Figure 17 - The cumulative of crack lengths versus the number of cycles for 4 specimens built in 45° angle of orientations.

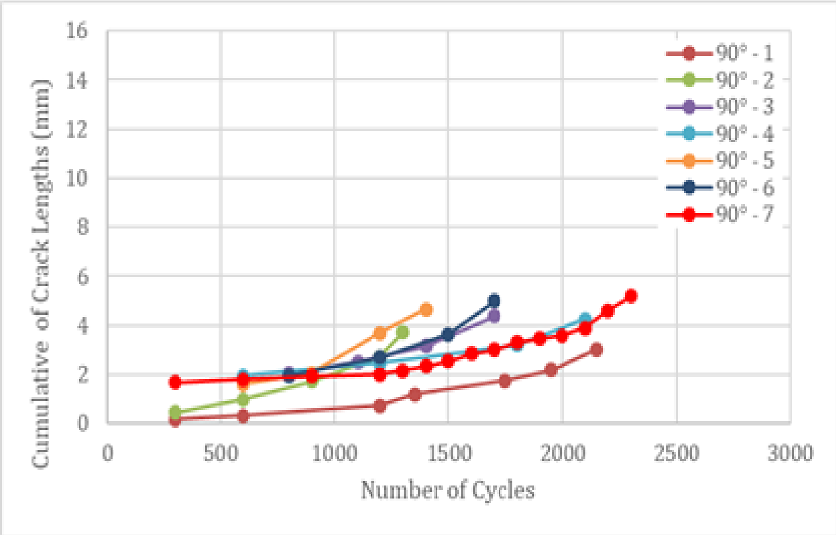

Figure 18 – The cumulative of crack lengths versus the number of cycles for 7 specimens built in 90° angle of orientations.

The effect of AM manufacture parameters on fatigue life of ABS polymer parts was investigated in [15]. The study demonstrated that layer build orientation and the direction of the printed polymer molecules on had a great impact on the fatigue life of AM components manufactured by FDM technique. In addition, it found that the air gaps within the printed sample which formed due to the manufacturing process plays a significant role in the fatigue life. The crack propagates much faster for a specimen that has a larger number of voids between the ABS filaments. The air gap locations and distributions can significantly affect the crack formation and consequently its propagation. In other words, as the fatigue testing on, the existing cavities and the formation of the voids will accelerate the crack and increase the rate at which it will eventually lead to final failure [31]. Several researchers evaluated the measuring process of fatigue crack [28]. The accuracy of crack measurements and the issues associated with the measuring methods was comprehensively discussed [32]. It was argued that any variation might be due to experimental scatter and test setup.

The relation between the cumulative crack lengths versus the number of cycles for specimens fabricated in 0°, 22.5°, 45°, 67.5°, and 90° is presented in Fig (19). The result demonstrates that the crack propagation for specimen built with 0° angle of orientation is considerably faster than the crack speeds of the other coupons. The crack growth for specimen manufactured in 67.5° orientation was found to the slowest among this group of specimens. As displayed in Fig (19), the exponential equations that represent each curve separately was identified using Excel's auto-generated curves.

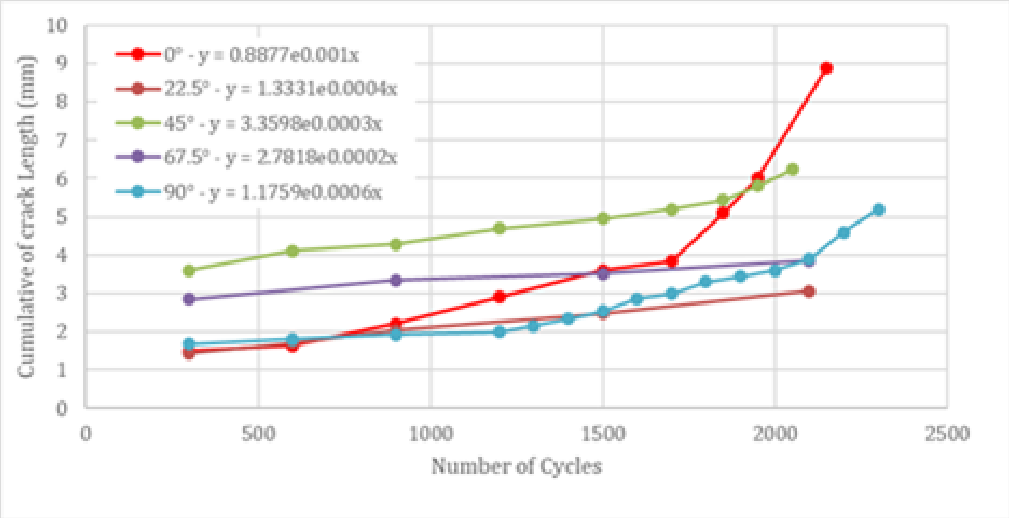

Figure 19 - The cumulative of crack lengths versus the number of cycles for specimens manufactured with (0°, 22.5°, 45°, 67.5°, 90°) orientations.

3.2 Limitations and Sources of Errors

An unavoidable source of error occurred during measurement as it was observed that the crack measurements methodology introduced a stress relaxation in the specimen which affects the fatigue life of AM polymer parts. The stress relaxation in the part is caused by subjecting the specimen to 300 fatigue cycles and then stopping the test to measure the crack lengths. To clarify, whenever the test is stopped, the stress on the specimen is reduced. Consequently, this stress relaxation leads to extended fatigue life of the AM polymer sample. To demonstrate the variation in fatigue life due to stress relaxation, 3 specimens with 0°, 45°, and 90° angles of orientations were tested under fatigue test. This experiment was conducted without stopping or even pausing the test. The final number of cycles at failure were recorded as the following:

- AM fatigue coupon oriented in 0° failed at 691 cycles
- AM fatigue coupon oriented in 45° failed at 760 cycles
- AM fatigue coupon oriented in 90° failed at 1090 cycles

By comparing this results with the previous result shows that a specimen cycling without stopping has one half or even a third of the fatigue life compared to the 300-cycle batching method. Therefore, the assumption of fatigue life variation being associated with stress relaxation was valid in this case. Although effort was dedicated to help align the specimens vertically using the fences, a 100% pure uniaxial fatigue tension was not expected to be able to achieve. The setup was closely examined and optimized to get complete uniaxial tension, but the results showed some effects of imperfect test setup on the fatigue life of AM polymer materials. Also, it is important to consider any pre-existing cracks in the crack region. It is very common for specimens to have a single crack surrounded by other cracks. Having such a natural phenomenon will influence the crack speed and consequently affect fatigue life. The existing of air gaps between the polymer filaments within a specimen will reduce the part's safe life. This is because during cyclic loading, those gaps will act as stress raisers which will help to increase the chance for crack nucleation which will shortly be followed by crack propagation. The current fatigue results in this study could be indicative of this crucial property of AM polymers.

5. Conclusion and Recommendations

The fatigue properties of ABS- P430 polymer specimens manufactured using FDM technique were experimentally investigated. The influence of the building orientation on the AM polymer part fatigue life was also investigated. The result showed a variation of fatigue life according to the build orientations. The specimens built with 0° orientation demonstrated a consistent fatigue behavior. The fatigue coupons failed within a range of cumulative crack lengths between 12 mm to 14 mm, and the fatigue life was recorded to be between 2050 to 2600 cycles. For fatigue part fabricated with 45° orientation, the cumulative cracks lengths were almost 50 % lower than the cumulative cracks lengths measurements for AM parts manufactured with 0° orientation. The fatigue life was recorded to be between 2000 to 2350 cycles. In case of the parts manufactured with 90° orientation, the cumulative crack lengths compared to other parts was found to be shorter by about 6 mm for all tested specimens. The fatigue life was recorded to be between 1300 to 2250 cycles. AM part manufactured with 90° has a better fatigue life in comparison with other specimens manufactured with 0°, 22.5°, 45°, and 67.5° orientations. It is essential when considering the build orientations versus the number of fatigue cycles as there should not be any directional effect within the machine. However, here there is indeed a directional bias when considering the build orientations versus the number of cycles. For safe life, it is recommended to design a part with the lowest present of the number of cycles. it is important that the infill raster orientation of AM parts must be considered in the design of components and this cannot be left uncontrolled as it will have a significant and difficult to predict effect on part life. Although the effect of layer thickness for the AM parts was not discussed in this paper, it is a part of larger ongoing research; the initial results recommend manufacturing AM polymer specimens with lower layer thickness. This will help reduce the air gaps, increasing the part density and consequently improve the fatigue life for AM polymer components.

6. References

[1] M. D. Monzón, Z. Ortega, A. Martínez, and F. Ortega, "Standardization in additive manufacturing: activities carried out by international organizations and projects," *Int. J. Adv. Manuf. Technol.*, vol. 76, no. 5–8, pp. 1111–1121, 2014.

[2] A. Boschetto and L. Bottini, "Accuracy prediction in fused deposition modeling," *Int. J. Adv. Manuf. Technol.*, vol. 73, no. 5–8, pp. 913–928, 2014.

[3] C. Weller, R. Kleer, and F. T. Piller, "Economic implications of 3D printing: Market structure models in light of additive manufacturing revisited," *Int. J. Prod. Econ.*, vol. 164, pp. 43–56, 2015.

[4] S. H. Huang, P. Liu, A. Mokasdar, and L. Hou, "Additive manufacturing and its societal impact: A literature review," *Int. J. Adv. Manuf. Technol.*, vol. 67, no. 5–8, pp. 1191–1203, 2013.

[5] S. H. Khajavi, J. Partanen, and J. Holmström, "Additive manufacturing in the spare parts supply chain," *Comput. Ind.*, vol. 65, no. 1, pp. 50–63, 2014.

[6] C. Lindemann, T. Reiher, U. Jahnke, and R. Koch, "Towards a sustainable and economic selection of part candidates for additive manufacturing," *Rapid Prototyp.*, vol. 21, pp. 216–227, 2015.

[7] G. J. Schiller, "Additive manufacturing for Aerospace," *IEEE Aerosp. Conf. Proc.*, 2015.

[8] L. Nickels, "AM and aerospace: an ideal combination," *Met. Powder Rep.*, vol. 70, no. 6, pp. 300–303, 2015.

[9] M. Marya, V. Singh, S. Marya, and J. Y. Hascoet, "Microstructural Development and Technical Challenges in Laser Additive Manufacturing: Case Study with a 316L Industrial Part," *Metall. Mater. Trans. B Process Metall. Mater. Process. Sci.*, vol. 46, pp. 1654–1665, 2015.

[10] D. Thomas, "Costs, benefits, and adoption of additive manufacturing: a supply chain perspective," *Int. J. Adv. Manuf. Technol.*, pp. 1857–1876, 2016.

[11] J. Scott, N. Gupta, C. Weber, and S. Newsome, "Additive manufacturing: Status and opportunities," *Sci. Technol. Policy Inst.*, pp. 1–35, 2012.

[12] A. A. Shapiro *et al.*, "Additive Manufacturing for Aerospace Flight Applications," vol. 53, no. 5, pp. 952–959, 2016.

[13] B. D. Rutkay, "A Process for the Design and Manufacture of Propellers for Small Unmanned Aerial Vehicles," MSc Thesis, Carleton University, 2014.

[14] C. W. Ziemian, R. D. Ziemian, and K. V. Haile, "Characterization of stiffness degradation caused by fatigue damage of additive manufactured parts," *Mater. Des.*, vol. 109, pp. 209–218, 2016.

[15] S. Ziemian, M. Okwara, and C. W. Ziemian, “Tensile and fatigue behavior of layered acrylonitrile butadiene styrene,” *Rapid Prototyp. J.*, vol. 21, no. 3, pp. 270–278, 2015.

[16] J. Furmanski and L. A. Pruitt, “Static mode fatigue crack propagation and generalized stress intensity correlation for fatigue–brittle polymers,” *Int. J. Fract.*, vol. 210, no. 1–2, pp. 213–221, 2018.

[17] J. Lee and A. Huang, “Fatigue analysis of FDM materials,” *Rapid Prototyp. J.*, vol. 19, no. 4, pp. 291–299, 2013.

[18] J. Laliberte, A. Dewar, B. Rutkay, and B. Hallgrimmson, “Measurement of Static Tensile Properties of 3D Printed Polylactic Acid (PLA) Using a Modified ASTM D638 Coupon Design Introduction.”

[19] R. P. Kambour, “A review of crazing and fracture in thermoplastics,” *J. Polym. Sci. Macromol. Rev.*, vol. 7, no. 1, pp. 1–154, 2003.

[20] M. B. Aviation, “POLYMER LANDING GEAR BUSHINGS CHALLENGE AVIATION ’ S STATUS QUO,” 2018. [Online]. Available: https://www.marshbrothersaviation.com/blogs/news/polymer-landing-gear-bushings-challenge-aviation-s-status-quo. [Accessed: 24-Mar-2019].

[21] Q. Z. Fang, T. J. Wang, and H. M. Li, “‘Tail’ phenomenon and fatigue crack propagation of PC/ABS alloy,” *Polym. Degrad. Stab.*, vol. 93, no. 1, pp. 281–290, 2008.

[22] R. Huang *et al.*, “Energy and emissions saving potential of additive manufacturing: the case of lightweight aircraft components,” *J. Clean. Prod.*, vol. 135, pp. 1559–1570, 2016.

[23] O. H. Ezeh and L. Susmel, “Fatigue behaviour of additively manufactured polylactide (PLA),” *Procedia Struct. Integr.*, vol. 13, pp. 728–734, 2018.

[24] Stratasys 3D printing company, “ABSplus-P430 Material Data Sheet,” 2017. [Online]. Available: http://usglobalimages.stratasys.com/Main/Files/Material_Spec_Sheets/MSS_FDM_ABSplusP430.pdf. [Accessed: 06-Mar-2016].

[25] J. J. Homan, “Fatigue initiation in fibre metal laminates,” *Int. J. Fatigue*, vol. 28, no. 4, pp. 366–374, 2006.

[26] J. C. Radon, “Fatigue crack growth in polymers,” *Int. J. Fract.*, vol. 16, no. 6, pp. 533–552, 1980.

[27] M. S. and S. Z. Constance Ziemian, “Anisotropic Mechanical Properties of ABS Parts Fabricated by Fused Deposition Modelling,” in *Intech open*, vol. 2, 2018, p. 64.

[28] E. E. Saenz, L. A. Carlsson, G. C. Salivar, and A. M. Karlsson, “Fatigue crack propagation in polyvinylchloride and polyethersulfone polymer foams,” *J. Sandw. Struct. Mater.*, vol. 16, no. 1, pp. 42–65, 2014.

[29] J. M. Barsom, *Fatigue-Crack Propagation in Steels of Various Yield Strengths*, vol. B73, no. 4. 1971.

[30] J. Wåle, “SKI Report 2006 : 24 Crack Characterisation for In-service Inspection Planning – An Update,” Inspecta Technology AB, 2006.

[31] S. Rabinowitz and P. Beardmore, “Cyclic deformation and fracture of polymers,” *J. Mater. Sci.*, vol. 9, no. 1, pp. 81–99, 1974.

[32] J. Kallrath, V. Altstädt, and J. P. Schlöder , “Analysis of fatigue crack growth behaviour in polymers and their composites based on ordinary differential equations parameter estimation,” *Polym. Test.*, vol. 18, no. 1, pp. 11–35, 1999.

Contact Author Email Address
Hayat El Fazani: hayatelfazani@cmail.carleton.ca

7. Copyright Statement